SCIENTIFIC PAPER JSLS

Magnetic Resonance–Visible Meshes for Laparoscopic Ventral Hernia Repair

Gernot Köhler, MD, Leo Pallwein-Prettner, MD, Oliver Owen Koch, MD, Ruzica Rosalia Luketina, MD, Michael Lechner, MD, Klaus Emmanuel, MD

ABSTRACT

Background and Objectives: We aimed to evaluate the first human use of magnetic resonance–visible implants for intraperitoneal onlay repair of incisional hernias regarding magnetic resonance presentability.

Methods: Ten patients were surgically treated with intraperitoneally positioned superparamagnetic flat meshes. A magnetic resonance investigation with a qualified protocol was performed on postoperative day 1 and at 3 months postoperatively to assess mesh appearance and demarcation. The total magnetic resonance–visible mesh surface area of each implant was calculated and compared with the original physical mesh size to evaluate potential reduction of the functional mesh surfaces.

Results: We were able to show a precise mesh demarcation, as well as accurate assessment of the surrounding tissue, in all 10 cases. We documented a significant decrease in the magnetic resonance–visualized total mesh surface area after release of the pneumoperitoneum compared with the original mesh size (mean, 190 cm^2 vs 225 cm^2; mean reduction of mesh area, 35 cm^2; $P < .001$). At 3 months postoperatively, a further reduction of the surface area due to significant mesh shrinkage could be observed (mean, 182 cm^2 vs 190 cm^2; mean reduction of mesh area, 8 cm^2; $P < .001$).

Conclusion: The new method of combining magnetic resonance imaging and meshes that provide enhanced signal capacity through direct integration of iron particles into the polyvinylidene fluoride base material allows for detailed mesh depiction and quantification of structural changes. In addition to a significant early postoperative decrease in effective mesh surface area, a further considerable reduction in size occurred within 3 months after implantation.

Key Words: IPOM, intraperitoneal onlay mesh, MR-visible meshes, PVDF.

INTRODUCTION

Laparoscopic ventral hernia repair was first introduced by LeBlanc and Booth[1] in 1993 and has established itself as a well-accepted option in the surgeon's armamentarium. Numerous studies have reported on the safety and efficacy of this approach. Above all, a shorter length of hospital stay and a decreased rate of complications—primarily wound infections—are documented compared with open procedures.[2] Meticulous technique and appropriate patient selection are critical to obtain the reported results because not every hernia is suitable for laparoscopic repair. The technique is limited regarding hernias that are large in width and associated with extensive visceral prolapse.[3]

Moreover, there is controversy regarding the mesh fixation technique among different kinds of tacks or transfascial sutures, and the existing literature does not show the superiority of one mesh fixation technique over the others regarding recurrence, whereas infection rates and pain increase when transfascial sutures are used.[4] Avoidance of metal tacks for fixation is recommended because of reported complications such as ileus and perforations.[5]

Another controversial point is whether fascial closure offers advantages over the original tension-free fascial gap bridging method regarding seroma formation, pseudorecurrence due to mesh bulging,[6] or more rapid peritoneal ingrowth in the presence of a potentially more suitable "landing plane."[7] Concern has also been raised over the fact that with the intraperitoneal onlay mesh (IPOM) technique, different composite or dually structured large ma-

Department of General and Visceral Surgery, Sisters of Charity Hospital, Linz, Austria (Drs. Köhler, Koch, Luketina, Emmanuel).

Department of Diagnostic and Interventional Radiology, Sisters of Charity Hospital, Linz, Austria (Dr. Pallwein-Prettner).

Academic Teaching Hospital, Medical University Graz, Graz, Austria (Drs. Köhler, Pallwein-Prettner, Koch, Luketina, Emmanuel).

Academic Teaching Hospital, Medical University Innsbruck, Innsbruck, Austria (Drs. Köhler, Pallwein-Prettner, Koch, Luketina, Emmanuel).

Department of Surgery, Paracelsus Medical University, Salzburg, Austria (Dr. Lechner).

Address correspondence to: Gernot Köhler, MD, Department of General and Visceral Surgery, Sisters of Charity Hospital, 4010 Linz, Austria. Telephone: +43 732 7677-0, Fax: +43 732 7677-7200, E-mail: gernot.koehler@bhs.at

DOI: 10.4293/JSLS.2014.00175

croporous implants are inserted directly into the peritoneal cavity and that, together with various methods of fixation, this could possibly give rise to complications such as bowel adherence and erosion, fistula formation, infection, mesh shrinkage, and migration through their direct contact with the viscera.[8–10] Surgical revision and removal of the implant are usually the consequence because conventional radiologic methods fail in precise visualization of common mesh types. Therefore noninvasive and reliable diagnostic tools are desirable. Experimental studies have reported on magnetic resonance (MR) visualization of surgical textile implants (STIs) loaded with superparamagnetic iron oxides—with and without positive-contrast susceptibility imaging—regarding delineation of meshes.[11,12] The first MR visualization of STIs in laparoscopic and open groin hernia treatment in humans has shown that iron-loaded implants can be accurately visualized in patients by means of magnetic resonance imaging (MRI) and that it is possible to assess mesh deformation in detail.[13] An experimental study dealt with visualization of MR-visible IPOM implants in a rabbit model and showed no significant reduction of mesh surface area after release of the pneumoperitoneum or in the later course of the trial with polyvinylidene fluoride (PVDF) meshes.[14]

We investigated the presentability of iron particle–loaded flat meshes inserted by a laparoscopic IPOM technique in humans for the first time. We aimed to assess both postoperative mesh deformation with the associated loss of total mesh surface area early after deflation of the pneumoperitoneum and mesh shrinkage 3 months postoperatively.

MATERIALS AND METHODS

With the informed written consent of our patients, we performed a prospective pilot series of 10 cases that was approved by the local ethics committee of our institution. Between December 2013 and February 2014, a total of 10 patients with midline incisional hernias were recruited for laparoscopic repair with MR-visible meshes at the Department of General and Visceral Surgery of the Sisters of Charity Hospital, Linz, Austria. Patients with non–MR-approved pacemakers, claustrophobia, or declared deficits in compliance with scheduled follow-up MR investigations were excluded.

Surgical Mesh Device

The Dynamesh IPOM implant (FEG Textiltechnik, Aachen, Germany) is a flat, large, macroporous (>1 mm) monofilament mesh, consisting of visceral-sided PVDF and parietal-sided polypropylene. We used quadratic meshes measuring 15 by 15 cm without additional trimming of the meshes. To provide MR visibility, tiny iron particles (Fe_3O_4 with iron load of 10 mg/g polymer) are embedded into the dark filaments of the base material and lead to local magnetic gradients between the mesh and surrounding tissue.

Surgical Technique

The surgical technique was rigorously standardized. The first port was inserted using Hasson's technique[15] at the level of the umbilicus on the left side of the abdomen as far lateral as possible. After insufflation of carbon dioxide up to a pressure of 12 mm Hg, 2 additional ports were inserted under direct laparoscopic control (5-mm port in left lower abdomen and 12-mm port in left upper abdomen, just below the costal arch). A complete adhesiolysis of the abdominal wall was then performed, and subsequently, the fascial defect was measured with a sterile intra-abdominal ruler after reduction of the pneumoperitoneum's pressure from 12 to 6 mm Hg (to avoid overestimation of the defect's real size). Needles were pricked through the skin at the borders of the hernia defect under laparoscopic control to assess the actual mesh position from outside the abdomen and to determine the ideal position of the transfascial sutures, which were placed at the very edges of the meshes. During implantation of the mesh over the fascial defect, we always aimed to keep the intra-abdominal pressure as low as possible. Because we consider a clear view of the surgical field at all times paramount for patient safety, the minimum intra-abdominal pressure during this part of the procedure was left to the operating surgeon's discretion. In any case, plane and smooth mesh placement to the peritoneum is absolutely required. At the edges, the implants were armed with 4 nonabsorbable monofilament sutures (No. 2–0 Prolene; Ethicon, Somerville, New Jersey) for transcutaneous and transfascial fixation with a suture passer. Further fixation was performed laparoscopically with absorbable strap devices (Secure straps; Ethicon) in a double-crown technique. The IPOM bridging technique without closure of the fascial defect was applied in all procedures (**Figure 1**).

Magnetic Resonance

On postoperative day 1 and at 90 ± 10 days postoperatively, all patients underwent MR examinations in a 1.5-T scanner (Symphony TIM; Siemens Medical Solutions, Malvern, Pennsylvania) using T1-weighted multishot gradient echo sequences (GREs) for detailed depiction of the configuration of the mesh implant. The surrounding tissue is represented as homogeneous and hyperintense and cannot be adequately assessed. T2-weighted turbo spin echo sequences are not

suitable for mesh depiction but are appropriate for precise delineation of the surrounding anatomic structures without interfering with mesh-related artifacts. MRI measurements were performed using sagittal, transverse, and coronal image analysis. The studies were performed in the supine position, the scans took 20 minutes to complete, and the slice thickness ranged from 2.5 to 5 mm.

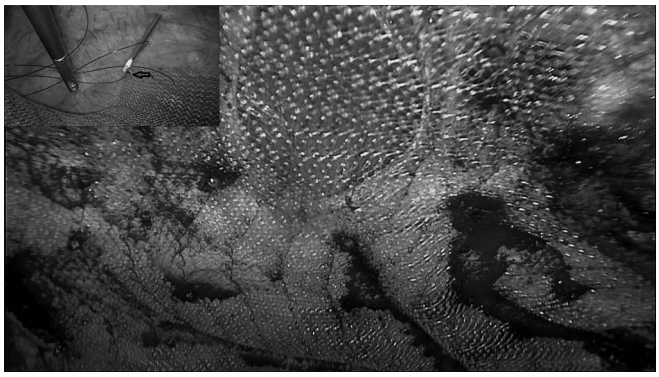

Figure 1. Standardized surgical technique: mesh placement with "bridging of the fascial defect." Fixation was performed with absorbable strap devices and nonabsorbable transfascial sutures placed at the very edges of the mesh (black arrow in inset).

Image Analysis

The trial's operating surgeon was excluded from the postoperative image analysis to avoid bias in the reports. Three of the authors reviewed the same blinded and representative images of every MR study independently after ideal image adjustment for each sequence protocol by the radiologist participating in the trial. The reviewers assessed the images independently according to the grading systems outlined in **Table 1**. After 3-dimensional reconstruction of all MR images, the total surface of the implanted meshes was explored and calculated with computer assistance (IntelliSpace image processing program; Philips Medical Systems, Andover, Massachusetts). The results were compared with the original mesh size to assess the decrease in mesh surface area after release of the pneumoperitoneum. The MR measurements taken 3 months postoperatively were compared with the original

Table 1.
Ratings of Independently Scored Images After Optimal Adjustment According to Sequence Protocol

	Image Analysis: MR[a] Sequence					
	General Appearance: 2D[a]-GRE[a]-T1 FLASH[a]	Conspicuity: 2D-GRE-T2* FLASH	Delineation: 2D-GRE-T1 FLASH	Surrounding Anatomic Structures: TSE[a]-T2 Blade	Amount of Folding: 2D-GRE-T1 FLASH	Hernia Overlap: 3D[a]-GRE-T1 VIBE[a]
Patient A	1.4	2.4	1.2	1	3.2	1.2
Patient B	1.2	1.6	1	1	2.8	1
Patient C	1.6	2.2	1.2	1.2	4	2.2
Patient D	1.2	2	1.4	1.2	3.2	1
Patient E	1.4	1.8	1.4	1	3	1
Patient F	1.2	1.8	1.6	1	3	1.2
Patient G	1.2	2	1.2	1.4	2.8	1
Patient H	1.4	2.2	1	1.2	4	1.2
Patient I	1.2	1.6	1.2	1	3	1
Patient J	1.2	1.2	1	1	3	1
Mean score for each criterion	1.3[b]	1.88[b]	1.22[b]	1.1[b]	3.2[c]	1.18[d]

[a]FLASH = fast low-angle shot; GRE = gradient echo sequence; MR = magnetic resonance; 3D = 3-dimensional; TSE = turbo spin echo sequence; 2D = 2-dimensional; VIBE = volumetric interpolated breath-hold examination.

[b]Scores were graded as follows: 1, excellent; 2, sufficient; 3, moderate; 4, insufficient; or 5, not at all.

[c]Scores were graded as follows: 0, not applicable; 1, no deformation; 2, mild deformation; 3, moderate deformation; or 4, severe deformation with loss of basic configuration.

[d]Scores were graded as follows: 0, not applicable; 1, hernia entirely covered with center of mesh; 2, hernia entirely covered but merely with periphery of mesh; 3, hernia partially covered; or 4, hernia not covered.

Table 2.
Demographic, Disease, and Surgical Parameters With Mesh Changes

	Age, y	Gender	BMI, kg/m^2	EHS[a] Classification[b]	Exact Fascial Defect Size, cm^2	Original Mesh Surface, cm^2	Mesh Surface Area on Postoperative Day 1, cm^2	Mesh Surface Area at 3 mo Postoperatively, cm^2
Patient A	81	Female	28.4	P: M2/W2	20	225	190	184
Patient B	58	Male	23.6	P: M2/3/W2	24	225	192	184
Patient C	58	Male	28.4	P: M3/W2	20	225	186	178
Patient D	74	Female	36.5	P: M3/W2	16	225	192	184
Patient E	84	Female	23.7	P: M2/W2	24	225	190	180
Patient F	56	Male	24.5	P: M3/W2	24	225	190	182
Patient G	39	Male	31.6	P: M3/W2	20	225	194	184
Patient H	49	Female	25.6	P: M2/W2	20	225	184	180
Patient I	57	Female	23.8	P: M3/W2	24	225	190	182
Patient J	81	Male	27.8	P: M2/W2	24	225	192	182
Mean	63.7 ± 15.31		27.39 ± 4.15		23.6 ± 4.78)	225	190; mean reduction, 35; $P < .001$	182; mean reduction, 43; $P < .001$

[a]EHS = European Hernia Society.

[b]EHS Classification of median ventral/incisional hernias: P = primary; R = recurrence; M1 = subxiphoid; M2 = epigastric; M3 = umbilical; M4 = infraumbilical; M5 = suprapubic; W1 = width <4 cm; W2 = width of 4 to 10 cm; W3 = width >10 cm.

mesh size and with the postoperative MR tomographic findings to assess further reduction of mesh size.

Statistics

Statistical analysis was performed with SPSS software for Windows (SPSS, Chicago, Illinois). All data are presented as mean ± standard deviation. We used the paired-samples *t* test to determine whether there is a significant difference between MRI-measured mesh dimensions and the original mesh size after testing for normal distribution with the Kolmogorov-Smirnov test. We considered *P* values of .05 or less to be statistically significant. The ratings for each criterion on the best suitable sequences, as well as patient demographic and disease characteristics, are presented with descriptive statistics.

RESULTS

Patient demographic and disease characteristics with relevant surgical parameters and mesh changes are outlined in **Table 2**.

By using the 2-dimensional GRE-T1 FLASH (fast low-angle shot) sequence, the mesh implant can be shown as a hypointense susceptibility artifact, visible as a distinct line of signal voids against hyperintense surrounding structures. The mesh itself is seen as a black structure because of its lack of water signals. The contrast to surrounding muscle and fatty tissue is clear (**Figure 2**), but it is difficult to distinguish the mesh from gas in the bowel. Nevertheless, the diagnostic quality regarding mesh configuration and delineation (ie, the possibility of assessing the correct position and overlap of the implant) was rated highest in the scoring system. All 10 implanted meshes were found in the same correct position in which they were placed during the operation and showed adequate overlap over the hernia defect of at least 5 cm to all sides.

Turbo spin echo–T2 Blade sequences cannot provide accurate depiction of the mesh, which is only displayed as a faint dotted line, but the surrounding anatomic structures are clearly visible. For the diagnostic quality regarding anatomy, this sequence received the highest rating.

Metallic-sensitive sequences (2-dimensional GRE-T2*) were not found to provide benefits. The mesh structure is oversubscribed as a conspicuously thick and dark depiction.

Three-dimensional GRE-T1 sequences turned out to have an unfavorable contrast-to-noise ratio but were rated as

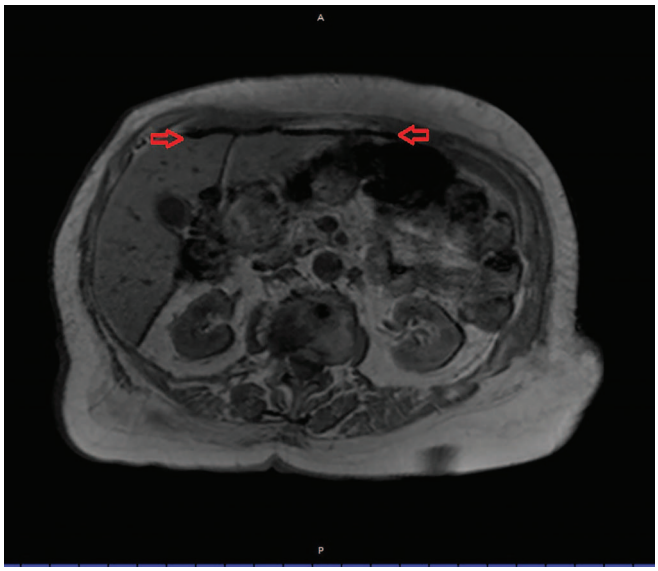

Figure 2. Two-dimensional GRE-T1 FLASH sequences provide precise mesh depiction (transverse image analysis). Arrows indicate the visible implant as a black line.

useful for measurements of the mesh surface and for evaluation of the overall mesh configuration. Three-dimensional reconstruction was used for calculation of the mesh surface area. The postoperative formation of wrinkles was moderate throughout but led to a significant reduction of the mesh surface areas as visualized in the MR studies when compared with the original sizes by the paired-samples *t* test. The mean reduction of MR-evaluated total mesh area was 15.6% and was thereby equivalent to a mean decrease of 35 cm^2. The remaining mesh surface for hernia defect coverage accounted for a mean of 190 cm^2, or 84.4% of the original mesh size of 225 cm^2 ($P < .001$). A precondition for correct comparability is accurate flat and smooth mesh placement during the operation, which could be achieved in all 10 cases. By comparing the amount of folding with the percentage of original mesh surface, an inverse correlation expectably can be observed: The more the mesh is wrinkled, the less surface can be measured, and vice versa. Three months postoperatively, the MRI findings showed significant reduction in effective mesh size (mean remaining mesh surface area, 182 cm^2; mean reduction of 8 cm^2, or 4.2%) compared with the measurements on the first postoperative day ($P < .001$). The difference between the original mesh size of 225 cm^2 and the mean calculated mesh surface area 3 months postoperatively (182 cm^2) was a mean of 43 cm^2, equivalent to 19.1% ($P < .001$). The results are summarized in **Table 2**.

DISCUSSION

The laparoscopic IPOM technique as used for the trial is basically a defect-bridging method without abdominal wall reconstruction. Therefore the mesh overlap has to be adequate to all sides to allow sufficient ingrowth and therefore permanent stability. Otherwise, a mesh bulged into the fascial defect by the intra-abdominal pressure can mimic a recurrent hernia.[6] Mesh folds or even deformations may work against peritoneal integration and ingrowth. To summarize, a smooth, wrinkle-free mesh placement with at least 5 cm of overlap to all sides and with only little tension on the mesh is required to achieve satisfactory results in patients.[3] Up to now, surgeons have only been able to assess correct mesh insertion intraoperatively, but laparoscopic mesh placement in the presence of the pneumoperitoneum with the associated distension of the abdominal wall may lead to overestimation of the real defect. After deflation, the collapse of the abdominal cavity leads to a reduction of circumference and, correspondingly, a relative surplus of mesh, which is suspected to result in considerable folding and mesh deformation. Therefore surgeons usually decrease the pneumoperitoneum when placing the implant over the fascial defect. However, this is limited because of the need for an unobstructed view during safe mesh placement and fixation. The results of a study investigating rabbits that had undergone laparoscopic IPOM repair of hernias showed no changes in total and effective mesh surface after release of gas,[14] but these findings seem not to be applicable to humans with an abdominal cavity at least 20 times larger, with different abdominal pressure ratios and a different abdominal wall anatomy. The difference between animal studies and human studies may also have to do with abdominal wall compliance. Regarding the findings in this trial, it appears that relevant changes in mesh configuration with a significant reduction of mesh surface definitely occur in humans after deflation of the pneumoperitoneum. However, we actually compared the surface measured postoperatively by MRI with the ex vivo surface. Formally, this does not show that these changes are only caused by the release of gas. Although the effect of mesh folding due to deflation is very likely, it seems not to be the only determining factor because the mesh surface could already be reduced by folds directly after implantation and while still in the presence of the pneumoperitoneum. Therefore, even with a significant result like the one found in this study, it would be inaccurate to conclude that the mesh surface reduction is only caused by the loss of the pneumoperitoneum. If the loss of the pneumoperitoneum were the only cause for mesh wrin-

kles and surface loss, one would estimate nearly the same degree in all patients. However, our results show differences of up to 10% loss of surface among the cases.

The position of all prostheses could be determined precisely, but it is not possible to distinguish between dense adhesions and only a loose contact of tissue structures with the mesh. Computed tomography (CT) was also considered to visualize iron-marked meshes and even provides better spatial resolution and higher-quality 3-dimensional reconstructed images than MRI. However, CT imaging does not work related to the tiny iron particles that lead to local magnetic gradients but do not give contrast for CT presentability.

Ciritsis et al[16] have reported that a significant mesh shrinkage of 20.9% occurred within 90 days after iron-loaded PVDF mesh implantation in inguinal hernia surgery. Regarding our study results, shrinkage and/or scarring in time led to a mean decrease in the mesh surface area of 19.1%, and this finding supports the demand for a wide overlap to all sides. Interestingly, the polypropylene-containing meshes used in our study showed no more but rather slightly less shrinkage compared with the pure PVDF meshes.[16] The proneness for shrinkage may be different owing to the mesh materials, as further investigations will show.

The results of an experimental study regarding IPOM in rats clearly showed that, in vivo and in vitro, the major decrease in mesh surface area due to shrinking was demonstrated between days 7 and 14, whereas after 21 days, it already seemed to narrow to a plateau.[17] Therefore the findings of our study 3 months postoperatively seem to provide reliable results in view of the definitive rate of mesh decrease. Further studies need to explore time-dependent findings and potential mesh alterations such as shrinkage, deformation, or migration in humans and correlate the results with clinical data. Perhaps MR visualization will not dramatically reduce revision surgery because the symptoms of the patients will certainly still guide the surgeon. MR-visible meshes probably can help to plan an intervention accurately because MR visualization of STIs offers a method by which to monitor such implants and should help to assess STI-related problems in a timely and precise manner. Furthermore, critical analysis of correct surgical technique and mesh placement is facilitated, and this may help to improve surgical skills, teaching procedures, and mesh designs.

We used a combination of PVDF and polypropylene meshes for better parietal ingrowth, and the additional parietal-sided incorporation of polypropylene into the base material did not compromise the MR depiction and demarcation of meshes. Maybe some mesh materials, compounds, or textures and designs will turn out to be useful or harmful. There is no evidence of the best type of mesh for laparoscopic IPOM, and the variety of materials available nowadays is enormous and hardly comprehensible. Furthermore, various bioprosthetics are pushed by industry and widely used despite an insufficient level of high-quality evidence in the literature.[18]

From our point of view, the diagnosis of a hernia recurrence usually justifies a reoperation on the one hand because of potential complications, which may be hernia or mesh material associated, and on the other hand because of an anticipatory further increase in recurrent hernia size. In our view, mesh bulging is a recurrence with an "expensive hernia sac" composed of mesh material and needs a revision just as if a "real" recurrence needs surgical correction. The surgical tactic and technique depend mainly on hernia localization and size, as well as surgical expertise. The results of our study indicate that we should be significantly increasing our mesh coverage of hernias because of potential shrinkage. Fundamentally, these studies should be repeated using several different mesh materials, but this is currently not feasible because of poor presentability of meshes in medical imaging. Mesh shrinkage is a key characteristic that we should be looking at when evaluating different mesh materials.

In conclusion, the results of our study clearly show that MR visualization of specially designed iron-loaded meshes is satisfactorily possible. A relevant postoperative decrease in the mesh surface area and further time-dependent mesh reductions owing to shrinkage and/or scarring could be demonstrated. The use of MR-visible meshes will probably help us to monitor implants and give answers to important questions in our daily clinical practice in view of potential changes in mesh characteristics and consequent complications.

The kind statistical support by Christian Steinlechner, MAg, is greatly acknowledged.

References:

1. LeBlanc KA, Booth WV. Laparoscopic repair of incisional abdominal hernias using expanded polytetrafluoroethylene: preliminary findings. *Surg Laparosc Endosc*. 1993;3:39–41.

2. Sajid MS, Bokhari SA, Mallick AS, et al. Laparoscopic versus open repair of incisional/ventral hernia: a meta-analysis. *Am J Surg*. 2009;197(1):64–72.

3. Bittner R, Bingener-Casey J, Dietz U, et al. Guidelines for laparoscopic treatment of ventral and incisional abdominal wall

hernias (International Endohernia Society (IEHS)—part 1. *Surg Endosc*. 2014;28(1):2–29.

4. Brill JB, Turner PL. Long-term outcomes with transfascial sutures versus tacks in laparoscopic ventral hernia repair: a review. *Am Surg,* 2011;77(4):458–465.

5. Sasse KC, Lim DC, Brandt J. Long-term durability and comfort of laparoscopic ventral hernia repair. *JSLS*. 2012;16(3):380–386.

6. Schoenmaeckers EJ, Wassenaar EB, Raymakers JT, Rakic S. Bulging of the mesh after laparoscopic repair of ventral and incisional hernias. *JSLS*. 2010;14(4):541–546.

7. Chelala E, Thoma M, Tatete B, et al. The suturing concept for laparoscopic mesh fixation in ventral and incisional hernia repair: mid-term analysis of 400 cases. *Surg Endosc*. 2007;21:391–395.

8. Seker D, Kulacoglu H. Long-term complications of mesh repairs for abdominal-wall hernias. *J Long Term Eff Med Implants*. 2011;21(3):205–218.

9. Mavros MN, Athanasiou S, Alexiou VG, et al. Risk factors for mesh-related infections after hernia repair surgery: a meta-analysis of cohort studies. *World J Surg*. 2011;35(11):2389–2398.

10. Fortelny RH, Petter-Puchner AH, Glaser KS, et al. Adverse effects of polyvinylidene fluoride-coated polypropylene mesh used for laparoscopic intraperitoneal onlay repair of incisional hernia. *Br J Surg*. 2010;97(7):1140–1145.

11. Kraemer NA, Donker HC, Otto J, et al. A concept for magnetic resonance visualization of surgical textile implants. *Invest Radiol*. 2010;45(8):477–483.

12. Kraemer NA, Donker HC, Kuehnert N, et al. In vivo visualization of polymer-based mesh implants using conventional magnetic resonance imaging and positive-contrast susceptibility imaging. *Invest Radiol*. 2013;48(4):200–205.

13. Hansen NL, Barabasch A, Distelmaier M, et al. First in-human magnetic resonance visualization of surgical mesh implants for inguinal hernia treatment. *Invest Radiol*. 2013;48(11):770–778.

14. Otto J, Kuehnert N, Kraemer NA, et al. First in vivo visualization of MRI-visible IPOM in a rabbit model. *J Biomed Mater Res B Appl Biomater*. 2014;102(6):1165–1169.

15. Hasson HM, Rotman C, Rana N, et al. Open laparoscopy: 29-year experience. *Obstet Gynecol*. 2000;96:763–766.

16. Ciritsis A, Hansen NL, Barabasch A, et al. Time-dependent changes of magnetic resonance imaging-visible mesh implants in patients. *Invest Radiol*. 2014;49(7):439–444.

17. Kuehnert N, Kraemer NA, Otto J, et al. In vivo MRI visualization of mesh shrinkage using surgical implants loaded with superparamagnetic iron oxides. *Surg Endosc*. 2012;26(5):1468–1475.

18. Bellows CF, Smith A, Malsbury J, Helton WS. Repair of incisional hernias with biological prosthesis: a systematic review of current evidence. *Am J Surg*. 2013;205(1):85–101.